Springer

Dear Author,

Here are the proofs of your article.

- You can submit your corrections **online**, via **e-mail** or by **fax**.
- For **online** submission please insert your corrections in the online correction form. Always indicate the line number to which the correction refers.
- You can also insert your corrections in the proof PDF and **email** the annotated PDF.
- For fax submission, please ensure that your corrections are clearly legible. Use a fine black pen and write the correction in the margin, not too close to the edge of the page.
- Remember to note the **journal title**, **article number**, and **your name** when sending your response via e-mail or fax.
- **Check** the metadata sheet to make sure that the header information, especially author names and the corresponding affiliations are correctly shown.
- **Check** the questions that may have arisen during copy editing and insert your answers/ corrections.
- **Check** that the text is complete and that all figures, tables and their legends are included. Also check the accuracy of special characters, equations, and electronic supplementary material if applicable. If necessary refer to the *Edited manuscript*.
- The publication of inaccurate data such as dosages and units can have serious consequences. Please take particular care that all such details are correct.
- Please **do not** make changes that involve only matters of style. We have generally introduced forms that follow the journal's style.
  Substantial changes in content, e.g., new results, corrected values, title and authorship are not allowed without the approval of the responsible editor. In such a case, please contact the Editorial Office and return his/her consent together with the proof.
- If we do not receive your corrections **within 48 hours**, we will send you a reminder.
- Your article will be published **Online First** approximately one week after receipt of your corrected proofs. This is the **official first publication** citable with the DOI. **Further changes are, therefore, not possible.**
- The **printed version** will follow in a forthcoming issue.

Please note

After online publication, subscribers (personal/institutional) to this journal will have access to the complete article via the DOI using the URL: http://dx.doi.org/[DOI].
If you would like to know when your article has been published online, take advantage of our free alert service. For registration and further information go to: http://www.springerlink.com.

Due to the electronic nature of the procedure, the manuscript and the original figures will only be returned to you on special request. When you return your corrections, please inform us if you would like to have these documents returned.

Metadata of the article that will be visualized in OnlineFirst

Please note: Images will appear in color online but will be printed in black and white.

ArticleTitle	Differential Response of the Urothelial V-ATPase Activity to the Lipid Environment	
Article Sub-Title		
Article CopyRight	Springer Science+Business Media, LLC (This will be the copyright line in the final PDF)	
Journal Name	Cell Biochemistry and Biophysics	
Corresponding Author	Family Name	**Calderón**
	Particle	
	Given Name	**R. O.**
	Suffix	
	Division	Primera Cátedra de Biología Celular, H. y E, Instituto de Biología Celular-Facultad de Ciencias Médicas
	Organization	Universidad Nacional de Córdoba
	Address	CC220, Ciudad Universitaria, 5000, Córdoba, Argentina
	Email	olga@cmefcm.uncor.edu
Author	Family Name	**Grasso**
	Particle	
	Given Name	**E. J.**
	Suffix	
	Division	Primera Cátedra de Biología Celular, H. y E, Instituto de Biología Celular-Facultad de Ciencias Médicas
	Organization	Universidad Nacional de Córdoba
	Address	CC220, Ciudad Universitaria, 5000, Córdoba, Argentina
	Email	
Author	Family Name	**Scalambro**
	Particle	
	Given Name	**M. B.**
	Suffix	
	Division	Primera Cátedra de Biología Celular, H. y E, Instituto de Biología Celular-Facultad de Ciencias Médicas
	Organization	Universidad Nacional de Córdoba
	Address	CC220, Ciudad Universitaria, 5000, Córdoba, Argentina
	Email	
Schedule	Received	
	Revised	
	Accepted	

Abstract The vesicle population beneath the apical plasma membrane of the most superficial urothelial cells is heterogeneous and their traffic and activity seems to be dependent on their membrane composition and inversely related to their development stage. Although the uroplakins, the major proteins of the highly differentiated urinary bladder umbrella cells, can maintain the bladder permeability barrier, the role of the membrane lipid composition still remains elusive. We have recently reported the lipid induced leakage of the vesicular content as a path of diversion in the degradative pathway. To extend the knowledge on how the lipid environment can affect vesicular acidification and membrane traffic through the regulation of the V-

	ATPase (vacuolar ATPase), we studied the proton translocation and ATP hydrolytic capacity of endocytic vesicles having different lipid composition obtained from rats fed with 18:1n-9 and 18:2n-6 fatty acid enriched diets. The proton translocation rate decreases while the enzymatic activity increases in oleic acid-rich vesicles (OAV), revealing an uncoupled state of V-ATPase complex which was further demonstrated by Western Blotting. A decrease of the very long fatty acyl chains length (C20–C24) and increase of the C16–C18 chains length in OAV membranes was observed, concomitant with increased hydrolytic activity of the V-ATPase. This response of the urothelial V-ATPase was similar to that of the Na–K ATPase when the activity of the latter was probed in reconstituted systems with lipids bearing different lengths of fatty acid chains. The studies describe for the first time a lipid composition-dependent activity of the urothelial V-ATPase, identified by immunofluorescence microscopy which is related to an effective coupling between the channel proton flux and ATP hydrolysis.
Keywords (separated by '-')	Urothelial vesicle acidification - V-ATPase specific activity - Membrane proton flux - Fatty acids
Footnote Information	

Journal: 12013
Article: 9172

Author Query Form

Please ensure you fill out your response to the queries raised below and return this form along with your corrections

Dear Author

During the process of typesetting your article, the following queries have arisen. Please check your typeset proof carefully against the queries listed below and mark the necessary changes either directly on the proof/online grid or in the 'Author's response' area provided below

Section	Details required	Author's response
Figure	Please indicate figure part labels (a, b) in Fig. 4 as it has been mentioned in the caption.	
	As per the information provided by the publisher, this article does not have colour figures in the print version. Hence, consider rephrasing the caption of Fig. 1.	

Cell Biochem Biophys
DOI 10.1007/s12013-011-9172-x

ORIGINAL PAPER

Differential Response of the Urothelial V-ATPase Activity to the Lipid Environment

E. J. Grasso · M. B. Scalambro · R. O. Calderón

Abstract The vesicle population beneath the apical plasma membrane of the most superficial urothelial cells is heterogeneous and their traffic and activity seems to be dependent on their membrane composition and inversely related to their development stage. Although the uroplakins, the major proteins of the highly differentiated urinary bladder umbrella cells, can maintain the bladder permeability barrier, the role of the membrane lipid composition still remains elusive. We have recently reported the lipid induced leakage of the vesicular content as a path of diversion in the degradative pathway. To extend the knowledge on how the lipid environment can affect vesicular acidification and membrane traffic through the regulation of the V-ATPase (vacuolar ATPase), we studied the proton translocation and ATP hydrolytic capacity of endocytic vesicles having different lipid composition obtained from rats fed with 18:1n-9 and 18:2n-6 fatty acid enriched diets. The proton translocation rate decreases while the enzymatic activity increases in oleic acid-rich vesicles (OAV), revealing an uncoupled state of V-ATPase complex which was further demonstrated by Western Blotting. A decrease of the very long fatty acyl chains length (C20–C24) and increase of the C16–C18 chains length in OAV membranes was observed, concomitant with increased hydrolytic activity of the V-ATPase. This response of the urothelial V-ATPase was similar to that of the Na–K ATPase when the activity of the latter was probed in reconstituted systems with lipids bearing different lengths of fatty acid chains. The studies describe for the first time a lipid composition-dependent activity of the urothelial V-ATPase, identified by immunofluorescence microscopy which is related to an effective coupling between the channel proton flux and ATP hydrolysis.

Keywords Urothelial vesicle acidification · V-ATPase specific activity · Membrane proton flux · Fatty acids

Abbreviations

V-ATPase	Vacuolar ATPase
AUM	Asymmetric membrane unit
ATP	Adenosine 5′-triphosphate
FITC	Fluorescein isothiocyanate
PK/LDH	Piruvate kinase/lactate dehydrogenase
NADH	Reduced nicotinamide-adenine dinucleotide
PEP	Phospho-enol-piruvate
CV	Control vesicles
LAV	Linoleic acid derived vesicles
OAV	Oleic acid derived vesicles
VLCFAs	Very long chain fatty acids
VLCPUFAs	Very long chain unsaturated fatty acids
LCFAs	Long chain fatty acids

Introduction

To investigate whether the urothelial endocytic vesicles acidification can be affected by the lipid environment, we studied both proton pumping and ATP hydrolytic activity of a V-ATPase present in the umbrella cells of urinary bladder whose membrane lipid composition was modified by dietary treatment. Both ATPase activities were differentially affected by oleic acid-rich diet compared with those of control and linoleic acid-rich diets.

E. J. Grasso · M. B. Scalambro · R. O. Calderón (✉)
Primera Cátedra de Biología Celular, H. y E, Instituto de Biología Celular-Facultad de Ciencias Médicas, Universidad Nacional de Córdoba, CC220, Ciudad Universitaria, 5000 Córdoba, Argentina
e-mail: olga@cmefcm.uncor.edu

Journal : Large 12013 | Dispatch : 19-2-2011 | Pages : 12
Article No. : 9172 | ☐ LE | ☐ TYPESET
MS Code : CBBI-D-10-00069 | ☑ CP | ☑ DISK

The urothelium, a specialized epithelium covering the lumenal surface of the urinary bladder mucosa is distinguished by two unique structural features of the superficial umbrella cells in direct contact with the urine [1], the asymmetric unit membrane (AUM) and the high density of cytoplasmic vesicles, rendering the urinary bladder a distinctive functional organ [2]. At least two kinds of subapical vesicles have been characterized: the discoidal/fusiform vesicles (FVs) and the peripheral junction-associated apical endosomes [3]. It has long been thought that FVs undergo fusion with the apical plasma membrane thus delivering crystalline plaques to the surface. The population of FVs can be restored by retrieval of membrane from surface of the umbrella cells. This mechanism has been documented to respond to the increase–decrease of hydrostatic pressure in the urinary bladder during the filling–voiding phases of the micturition cycle [2, 4]. The FVs membrane recycling has been questioned on the basis of the results suggesting that FVs can be regarded as exocytic rather than endocytic vesicles delivering uroplakins, the major protein of the surface membrane, to the apical plasma membrane [5–7]. The peripheral junction associated vesicles proceeds from an apical membrane compensatory endocytosis [3] and represent an integrin-regulated and RhoA-and dynamin-dependent pathway. These membrane and fluid internalized were targeted to lysosomal degradation [3]. This fate was not the classical lysosomal pathway, since the internalized membrane and fluid material were delivered to the junction-associated vesicles and not to FVs or classical early endosomes, and the fate of the cargo was the degradation in late endosomes/lysosomes. Others authors provide evidences that membrane-bound endocytotic marker after endocytosis is sorted to early endosome compartment which matures in late endosome and lately in lysosome [7]. Zhang et al. [8] also gave evidences of the vesicle pathway toward the lysosomal degradation demonstrating the surface characteristic AUM structure in multivesicular bodies, autophagosomes, and lysosomes of umbrella cells. Truschel et al. [9] have also reported that once the vesicles have been endocytosed, their membrane protein content, specifically the uroplakin III, could be degraded via lysosomes. Guo et al. [5] have recently demonstrated the acidification of the endocytic vesicle content and its dependence of Vps33a, a Sec-1 related protein implicated in vesicular transport to the lysosomal compartment. The toxins/inflammatory substances eliminated by urine may have a key role in the urinary bladder cancer development. This prompted to investigate the membrane permeability [10] and the ATPase-dependent acidification of the uroepithelial subapical endocytic vesicles to get insight into possible mechanisms of urinary bladder cancer development induced by urine content. On the basis of the previous data on the biochemical, biophysical, and structural analysis of these vesicles [10–14], we suggested that some membrane lipid changes, may not only induce a loss of the proper membrane organization but also a lipid-dependent lumenal content leakage toward the cytoplasm [10].

Whatever the endocytosed material proceeds it is finally targeted to the late endosome/lysosomal compartment where the cargo is degraded [3, 7]. The endosomal interior becomes acidified due to the presence of a Vacuolar proton-ATPase pump (V-ATPase, EC 3.63.14) [15]. This V-ATPase controls the cytoplasmic and extracellular pH as well as the acidity of diverse intracellular compartments, besides other functions such as the cellular energetic metabolism, intracellular membrane traffic, protease activity, vacuole-vacuole fusion, metal homeostasis, and cytoskeletal and morphological changes [15]. The acidification of the umbrella cell compartments that presumably belong to the lysosomal pathway has already been shown, thus implying the presence of a proton- pump that was demonstrated by immunofluorescence microscopy [16]. The V-ATPase is composed of two multisubunit domains: the membrane proton channel V_0, responsible for proton translocation, and the peripheral catalytic sector V_1, where the ATP hydrolysis occurs [17]. It has also been reported that the reversible physical disassembly of V-ATPase, into V_1 cytoplasmic and V_0 intramembrane segments may affect the normal functioning of the enzyme. Nevertheless, even after the correct association of intra and extra membrane subunits, a functional uncoupling can occur [17]. The mechanism underlying this type of uncoupled state is unclear. Although it could be assumed that the transmembrane V_0 subunit can be affected by the lipid environment, this has only been proven in a reconstituted system [18]. With this system, it was demonstrated that phospholipids are not essential for the basic ATP hydrolysis but rather are required for the functional coupling of the enzyme. Moreover, some dependence of the V-ATPase on the sphingolipids of the peripheral V_1 unit rather than on the integral segment V_0 has been noted [19]. The dependence of the lysosomal pathway on the acidification processes is quite clear. However, what remains unknown is whether different acidification grades could have a key role for determining the directionality (pathway sorting) to one or the other pathways occurring in the urinary umbrella cells. The proton translocation (proton-pumping) across biological membranes is driven by ATP hydrolysis which in turn leads to the rotation of the V_1 domain. This means that the proton translocation efficiency is dependent on the coordination between both functions [17]. So far, the coordination state between ATPase activity and proton translocation of the urinary bladder V-ATPase has not yet been studied. To elucidate this intriguing aspect, we studied first the V-ATPase functionality in different membrane

Journal : Large 12013 Dispatch : 19-2-2011 Pages : 12
Article No. : 9172 LE TYPESET
MS Code : CBBI-D-10-00069 CP DISK

organizations induced by changes of the membrane lipid composition, using the diet protocol reported earlier [10–14]. As an approach to understand how the mechanism of organelle acidification could be affected by the membrane environment we prepared urothelial endocytic vesicles of varied membrane lipid composition from bladders of rats fed with a commercial diet (control vesicles, CV) and synthetic diets enriched in 18:1n-9 (oleic acid-rich vesicles, OAV) and 18:2n-6 (linoleic acid-rich vesicles, LAV) fatty acids. The data presented in this study on those diet-conditioned urothelial vesicles provide evidences, using an endocytotic compartment of well characterized membrane lipid composition, that the specific activity of the proton-pump and the association/assembly of the two subunits, V_0 and V_1, are lipid regulated processes. We have chemically characterized for the first time the V-ATPase activity/proton translocation coupling in rat urothelium by studying its differential functional state, relative to the lipid environment, and we have additionally described some new regulatory mechanisms based on common daily nutrients.

Materials and Methods

Animals and Diets

After weaning, three groups of Wistar rats (both sexes), 25 each were fed ad libitum for 12 weeks with semi-synthetic formulae containing (% w/w) 20.0 casein, 50.0 sucrose, 20.0 corn starch, 3.5 salt mixture, 1.0 vitamins mixture, 0.3 methionine, 0.1 choline, and 6% of one of the following lipid sources: corn oil, enriched in 18:2n-6; and olive oil, enriched in 18:1n-9 [10]. Another group was fed with commercial animal diet (Cargil, Co) and used as a control. Food and water were provided ad libitum. Animals were kept in a light and temperature controlled room under the rules of the Institutional Animal Care Guidelines (Animal Care Comittee from National University of Cordoba, Argentina) and were fed fresh diet every day.

Identification of Urinary Bladder V-ATPase by Immunofluorescence

Rat bladders were fixed in 4% paraformaldehyde, embedded in paraffin and sectioned (3 μm thick slides). After deparaffinization and rehydration, the sections were blocked with 10% normal bovine serum in phosphate buffered saline (PBS), pH 7.4 for 1 h at room temperature. After blocking, the slides were incubated with primary antibody V-ATPase B1/2 (Santa Cruz Biotechnology, Inc) 1:50 at 4°C overnight. Anti-Rabbit Ig FITC conjugated (Sigma, Co) 1:200 as secondary antibody was used. The slides were mounted using DPX medium (Sigma, Co). Confocal images were collected using a Carl Zeiss LSM5 Pascal laser scanning confocal microscope (Carl Zeiss AG, Germany) equipped with a multi-line Argon laser (458, 488, and 514 nm) and two Helium Neon lasers (543 and 633 nm, respectively) and 100× (numerical aperture = 1.4) oil immersion objective (Zeiss Plan-Apochromat). Single confocal sections of 0.7 μm were taken parallel to the coverslip (xy sections). Final images were captured on a Zeiss mochromatic CCD camera and compiled with Adobe Photoshop 7.0.

Isolation of Urothelial Endocytic Vesicles and Determination of V-ATPase Proton Translocation

Two animals were used for each experiment. Ureters and urethra were ligated in situ after bladder exposure. The bladder interior was washed three times with phosphate-buffered saline at 37°C and then filled with 10 mM HEPES buffer, pH 7.5 containing 30 mM HPTS (hydroxypyrene-1,3,6-trisulfonic acid, Sigma Co) a pH-sensitive probe [20]. The bladders were removed and quickly exposed for 60 min to wormed Ringer hypotonic solution (in mM: 111.2 NaCl, 25 $NaHCO_3$, 5.8 KCl, 2 $CaCl_2$, 1.2 $MgSO_4$, 1.2 K_2HPO_4, 11.1 glucose, pH 7.4; diluted 1:1 with distilled water) which induces reinsertion of subapical vesicles to the membrane surface [21]. Immediately, the bladders were changed to an isotonic Ringer solution for 20 min to induce the endocytosis of plasma membrane entrapping the pH sensitive probe [10, 21]. This procedure mimics the protocol of Lewis and de Moura [22] designed to induce maximal reinsertion and endocytosis of apical plasma membrane successively. The remaining dye in the bladder interior was drained and the cavity rinsed several times with phosphate-buffered saline (PBS) at 4°C. The bladders were cut open on an ice-containing dish and the urothelium was obtained by scraping the lumenal surface, collected by centrifugation and mechanically disrupted in homogenization solution (in mM: 10 *N*-2-hydroxyethylpiperazine-*N*-2-ethanesulfonic acid, 10 KCl, 45 sucrose, 1 EDTA, 1 ethylene glycol-bis(2-aminoethyl ether)*N*,*N*,*N*,*N* tetracetic acid, pH 8). The disrupted tissue was layered over a 1.6 M sucrose cushion [10, 21] and centrifuged at 28,000×*g* at 4°C for 20 min in a L5-50B Beckman Ultracentrifuge. The urothelial vesicle-enriched fraction was collected at the water-sucrose interface and immediately assayed. The suspension of HPTS-loaded urothelial endocytic vesicles in saline solution was placed in a fluorometer cuvette and 5 mM each of Na^+-ATP and $ClMg_2$ or 5 mM each of Na^+-ATP and $ClCa_2$ was added (0 time). The fluorescence signal was measured (Farrand Mk I-FOCI equipped with a magnetic stirrer) at the emission wavelength of 515 ± 3 nm (excitation wavelength 450 ± 5 nm) and registered

Journal : Large 12013 Dispatch : 19-2-2011 Pages : 12
Article No. : 9172 LE TYPESET
MS Code : CBBI-D-10-00069 CP DISK

every 5 min using a time-window device. The integrity of the loaded vesicles was always tested by treatment of a separate aliquot with Triton X-100 (0.2%) and measuring the increase of the fluorescence upon dilution that follows the release of the trapped self-quenched pH sensitive probe. All vesicles were loaded with the same buffer and amount of HPTS fluorescent probe (30 mM). A calibration curve of fluorescence emission intensity ratios (λ_{Ex450} and λ_{Ex} 403) as a function of pH was constructed using the fluorescence spectra of the HPTS [20]. These F_{Em} ratios are useful in reporting physiological pHs (4.5–7.4) and were used to control the initial pH and pH changes during the experimental time. The initial intravesicular pH was essentially identical (6.5–6.8) in all vesicle samples and the pH changes were within the sensibility range of the probe (unpublished results). All fluorescence measurements (arbitrary units, A.U.) were normalized to 100 µg protein and expressed as percentage of the value at 0 time (range 38–40 A.U.) taken as 100%.

ATP Hydrolytic Activity of Urothelial Endocytic Vesicles V-ATPase

Two to three animals for each experiment were euthanized, the bladders were cut opened, and urothelium and vesicles were isolated as described above. The V-ATPase activity was continuously assayed in triplicate at 37°C, using a PK/LDH linked system in which the hydrolysis of ATP was coupled to the oxidation of NADH [23]. The reaction was monitored (oxidation of NADH) at 340 nm (ε_{340nm} = 6200 M^{-1} cm^{-1}, pH 7.5) in a Hitachi U-2000 spectrophotometer equipped with thermostatic cell holders. For the standard reaction, the vesicles were suspended in 50 mM HEPES buffer, pH 7.5, containing 3 mM ATP, 10 mM KCl, 5 mM $MgCl_2$, 50 mM NaCl, 0.14 mM NADH, 2 mM PEP, 205 µg PK (123 U), and 275 µg LDH (236 U) in a final volume of 1.0 ml [23]. The decrease of the absorbance value at 340 nm was registered and the increments at each time were expressed as follow:

$$\Delta Abs = Abs_0 - Abs_t$$

where Abs_0 corresponds to the initial absorbance and Abs_t the absorbance measured at subsequent times. By using the extinction coefficient (ε_{340nm} = 6200 M^{-1} cm^{-1}) and the absorbance changes, the nmoles of ATP hydrolyzed were obtained. The ATP hydrolysis due to the presence of P-ATPases such as Na–K ATPase was inhibited by previous incubation of the enzymatic system with ouabain and sodium orthovanadate (5 mM and 3 µM, respectively) for 1 h. The mitochondrial F-ATPase was removed during the centrifugation process. The background activity (determined in the absence of ATP) was subtracted from all of the values shown.

Distribution and Quantification of V-ATPase by Immunoblotting

Six rat bladders for each experiment were cut opened and the vesicular enriched fraction was obtained from the scraped urothelium, after centrifugation on a sucrose cushion as described above. The sucrose-free-upper phase, including the endocytic vesicle containing interphase, was carefully separated and centrifuged at 100,000×g at 4°C for 90 min in a L5-50B Beckman Ultracentrifuge. Thus, the vesicular membrane associated V-ATPase (pellet) and the cytosolic domain (supernatant) were isolated. Both fractions isolated were submitted to Western-blotting to detect the B subunit of the V_1 domain. To this purpose, the fractions were separately treated as follow: the vesicular membrane fraction was solubilized in cracking buffer (8 M urea, 5% SDS, 1 mM EDTA, 50 mM Tris–HCl, pH 6.8, 5% β-mercaptoethanol) [24] and the supernatant (cytosolic fraction) was precipitated with 10% trichloroacetic acid, centrifuged at 10,000×g and the pellet solubilized with cracking buffer [24]. Both preparations were kept apart for immunoblotting analysis. Parallelly, sections of renal cortex were incubated in lysis buffer (1 ml per 1 mg of tissue) containing: 150 mM NaCl, 1.0% triton X-100, 50 mM Tris, pH 8.0 and 1 mM EDTA, 1 mM EGTA, 1 mM Leupeptin, and 50 µM SPMF as protease inhibitors for 30 min at 4°C and homogenized. The homogenate was centrifuged at 10,000×g at 4°C for 10 min. The supernatant containing the solubilized V-ATPase of renal tubules was used as positive control. All preparations were run on SDS-PAGE 7.5% and the resolved proteins bands were electrophoretically transferred to nitrocellulose membranes (Immobilon-NC, Millipore Co) for 1 h at 300 mA. After blocking with 0.5% Non Fat Milk/TBS for 1 h at room temperature, the membranes were incubated with V-ATPase B1/2 antibody 1:200 overnight at 4°C. After washing, the membranes were incubated with HRP-conjugated anti-Rabbit secondary antibody (Santa Cruz Biotechnology Inc.) 1:500 and the specific protein bands were developed with H_2O_2–DAB (Sigma Co.). The relative amount of individual bands was calculated using the computer software Sigma Scan Pro 5.0 (Spss Inc. 1987–1999) on scanned films.

Fatty Acid Determination

Total lipids from vesicle membranes were extracted according to Folch method [25]. Dried total lipid extracts were treated with toluene (500 µl) and sodium methoxide (1 ml, 0.5 M) at 4°C overnight [26]. The fatty acid methyl esters were extracted with hexane and the fatty acid profile was identified using a gas chromatographer (Perkin Elmer, Waltham, USA) equipped with a capillary column. (BPX

Journal : Large 12013 Dispatch : 19-2-2011 Pages : 12
Article No. : 9172 LE TYPESET
MS Code : CBBI-D-10-00069 CP DISK

70.30 m length, ID 0.25 mm, film 0.25 μm, Phenomenex, Torrance, USA). The temperature for the injector and detector was 280°C, and the oven temperature was maintained at constant temperature (190°C). The fatty acids were identified using commercial standards and expressed as percentage of total fatty acid composition. Organic solvents, such as chloroform, methanol, hexane, sodium methoxide, and reagents, were provided by Sigma Chemical Co.,St. Louis, USA and FA standards by Nu-Check Prep Inc., Elysian, USA.

Protein Determination

All protein determinations were according to Lowry et al. [27].

Statistical Analysis

All results are expressed as average of at least three independent experiments. Data obtained were statistically analyzed by ANOVA-Bonfferoni test and a level of less than $P < 0.05$ was chosen to detect significant differences using the statistical software InfoStat Professional version 1.1.

Results

Identification of Urinary Bladder V-ATPase by Immunohistochemistry

The presence of vacuolar ATPases (ATP-driven proton pumps) has been identified in the plasma membrane of the lower urinary tract [16] by fluorescence and electron microscopy. We now report the presence of an urothelial V-ATPase in three rat urinary bladder urothelia with different membrane lipid composition. The study revealed that the V-ATPase was concentrated in both the plasma membrane and cytoplasmic compartments of the umbrella cells layer (Fig. 1). No labeling of intermediate and basal layers was detected indicative of the absence of the V-ATPase in most internal zones of bladder mucosa.

The Proton Transport Activity of Urinary V-ATPase in Presence of Mg^{2+} and Functional Uncoupling in Presence of Ca^{2+}

The vacuolar-type V-ATPases transports protons either from the cytoplasm to the extracellular space or from the cytoplasm to the endomembrane system where the resulting acid pH is essential for the organelle functions. To elucidate the dependence of V-ATPase enzymatic function on the vesicular membrane lipid composition, we followed the dynamics of proton transport across the membrane of uroepithelial endocytic vesicles of different membrane lipid composition. These vesicles, isolated by differential centrifugation from the urothelium homogenate, have been characterized earlier as cytoplasmic endocytic vesicles by biochemistry and electron microscopy studies that revealed a prominent presence of superficial uroplakin-containing plaques [2, 4, 14]. The vesicles were loaded by endocytosis with HPTS, a pH-sensitive probe whose fluorescence emission at 520 nm (excitation 450–470 nm) [20] decreases as a result of reversible proton binding. The HPTS fluorescent pH indicator has been used for measuring the intraorganelle pH in the endosomal–lysosomal pathway in neurons [28] and to follow the endocytic pathway of liposome-delivered HPTS in cultured kidney cells [20]. This fluorescent dye has a pK_a of 7.3 and responds with high sensitivity to changes in pH regardless of organelle size or dye concentration. It is membrane impermeant preventing escape across biological membranes. Compressively HPTS has been recognized as the most useful probe for measuring pH at the physiological range (4.5–7.6) [28]. This singular property of HPTS allows to follow the proton transport across the vesicle membrane. The fluorescence changes registered correspond to the HPTS localized in the vesicle interior, since once the probe has been internalized by endocytosis, it does not cross the vesicle membrane due to its high negative charge. The fluorescence registered after the addition of the substrate (ATP) and the cofactor (Mg^{2+}) decreased to approximately 50% of the initial value at 5 min after the starting reaction, both in commercial diet-derived vesicles (CV) and in the corn oil-diet derived vesicles (LAV) (Fig. 2). However, the fluorescence decrease in the olive oil-diet derived vesicles (OAV) was slower and reached similar values to that of the control only after 25 min of the ATP and Mg^{2+} addition. With the addition of Ca^{2+}, the fluorescence decrease was smaller in CV and LAV being almost the same as with Mg^{2+} in OAV. The latter values, due to processes other than the V-ATPase proton translocation, were subtracted from those reached in presence of Mg^{2+} thus obtaining the "true" V-ATPase proton translocation activity: "true" V-ATPase $= \Delta F_t(Mg^{2+}) - \Delta F_t(Ca^{2+})$. The fluorescence changes were normalized to 100 μg protein and expressed as percentage of the corresponding values at 0 time (Fig. 2).

ATP Hydrolytic Activity of V-ATPase of Urothelial Endocytic Vesicles

The ATP hydrolytic activity of V-ATPase in fatty acid enriched endocytic vesicles was determined by continuously measuring the oxidation of NADH in the PK/LDH linked system. The absorbance decrease at 340 nm due to the oxidation of the NADH was expressed as the

Journal : Large 12013 Dispatch : 19-2-2011 Pages : 12
Article No. : 9172 LE TYPESET
MS Code : CBBI-D-10-00069 CP DISK

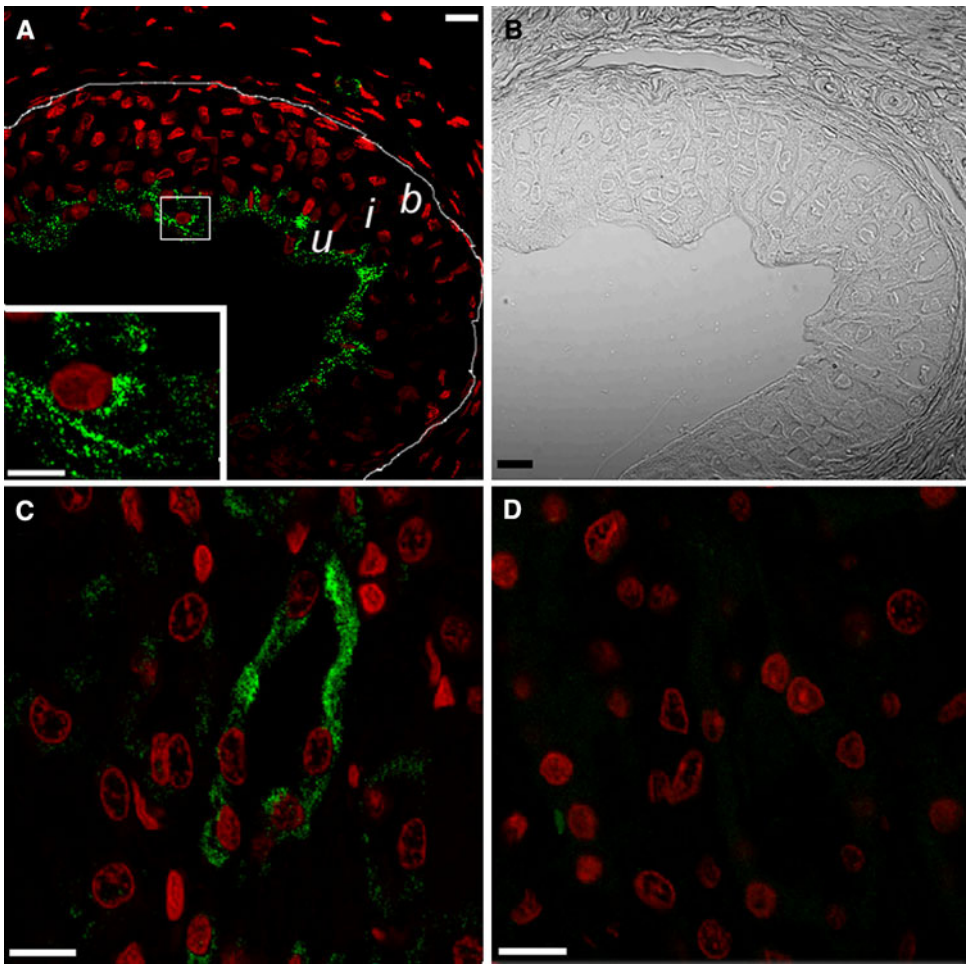

Fig. 1 Detection of urinary bladder V-ATPase by immunofluorescence. Sections of fixed rat urinary bladder were blocked and incubated with primary antibody V-ATPase B1/2 (1:50) at 4°C overnight. Anti-Rabbit Ig FITC conjugated (1:200, exc 488 nm) as secondary antibody was used. The slides were mounted and examined with an LSM5 Pascal Confocal Microscope). **a** the image shows the three layers of bladder mucosa: the superficial umbrella cells (*u*), intermediate cells (*i*), and basal cells (*b*).The presence of the V-ATPase (*green* positive labeling) is viewed in the umbrella cell layer. No positive signal was seen in the other two internal layers (*i*) and (*b*) denoting the lack of the enzyme. The nuclei were stained with propidium iodine, exc 546 nm; *inset* digital zoom of the zone marked (10 X). *Line* indicates the basal membrane limit. **b** phase contrast of **a. c**, **d** sections of renal cortex (positive control) with (**c**) and without (**d**) primary antibody. Similar results were observed in LAV and OAV. *Bars* 10 μm, magnification 1000×, immerse oil objective 100× NA 1.4

increments measured at each time, and were taken to determine the V-ATPase specific activity of each type of vesicles studied (Fig. 3). The results showed that in the case of OAV the hydrolysis of ATP (0.34 ± 0.023 nmoles/μg prot/min) was 13.8 times higher than CV and LAV (0.024 ± 0.004 and 0.02 ± 0.009 nmoles/μg prot/min, respectively). The anomaly showed by V-ATPase in OAV, where the ATPase activity did not parallel the rate of proton translocation but rather increased with higher slope than that of the proton movement, suggests a deficient coupling between V_0 and V_1 domains of the enzyme complex. Two probable determinant factors of the coupling/uncoupling state, the physical dissociation (assembled/dissembled) and the functional uncoupling of V_0 and V_1 domains were studied. The coupling state was assayed with two different approaches: first, the proton translocation in presence of either Mg^{2+} (coupled state) or Ca^{2+} (uncoupled state) was measured as mentioned above. Second, to assess the physical association of the two domains V_0 –V_1, the cytosolic V_1 domain was followed by performing immunoblotting assays probing the subunit B of the V_1 domain with the V-ATPase B1/2 antibody. As illustrated in Fig. 4, we found the presence of the B subunit always associated to the membrane fractions of the endocytic vesicles. Absence of the B subunit in the soluble cytosolic fraction of all three membranes studied was routinely observed. Note that soluble cytosolic fraction is referred to the microsomal fraction obtained at 100,000×*g* and may contain vesicles smaller than 0.5 nm.

Journal : Large 12013 Dispatch : 19-2-2011 Pages : 12
Article No. : 9172 ☐ LE ☐ TYPESET
MS Code : CBBI-D-10-00069 ☑ CP ☑ DISK

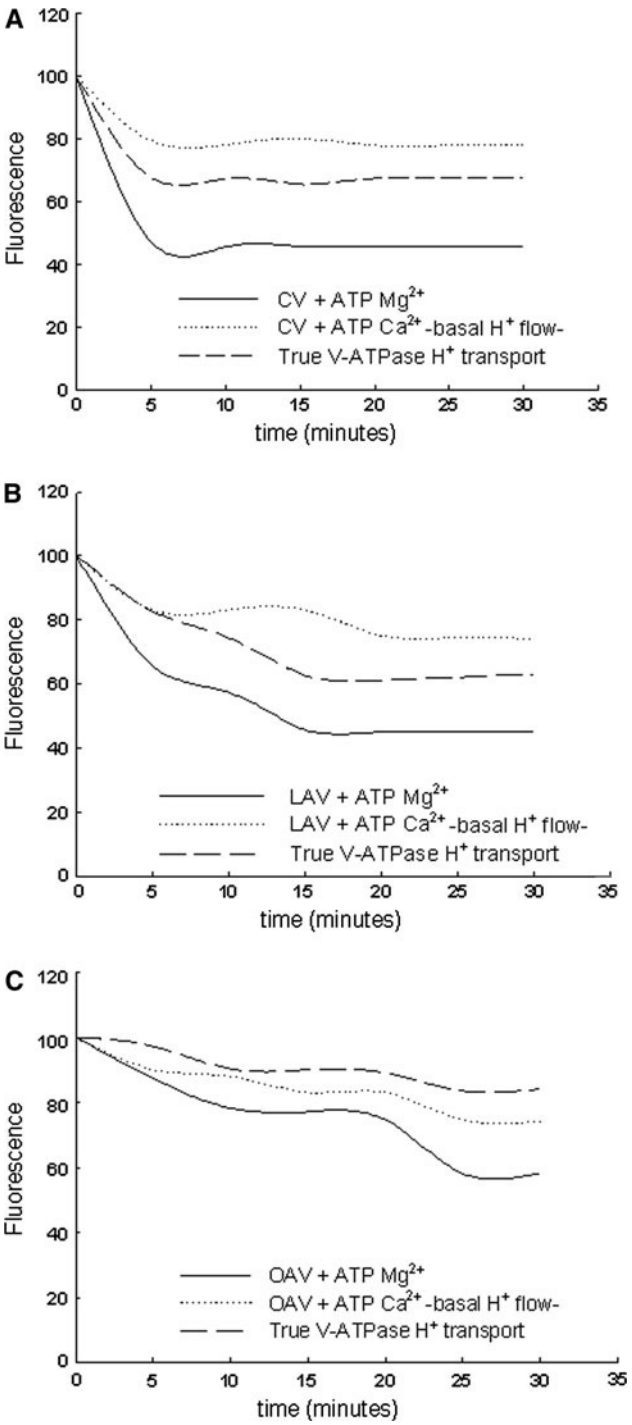

Fig. 2 Acidification of the endocytic vesicle lumenal content. Endocytic vesicles loaded with HPTS, a pH sensitive fluorescence probe, were isolated by centrifugation (see "Materials and Methods"). The vesicle suspension was incubated at 37°C with Na-ATP and, after the addition of either Mg^{2+} or Ca^{2+} (5 mM each), the fluorescence emission was registered for the indicated time. The results are expressed as percentage of the value at 0 time taken as 100%. **a** CV, **b** LAV, **c** OAV. A decrease of approximately 50% of fluorescence emission was observed in CV and LAV due to HPTS protonation in the presence of Mg^{2+}. The acidification was slower in OAV, reaching values similar to CV only after 25 min ($P < 0.05$). When Ca^{2+} instead of Mg^{2+} was added, the fluorescence decrease was lower indicating the uncoupled V-ATPase state (impaired proton translocation) induced by this cation. When the V-ATPase was uncoupled by the presence of Ca^{2+}, the fluorescence decay is taken as the kinetic of the proton permeability in absence of V-ATPase activity. The true V-ATPase proton translocation was expressed as the Δ fluorescence in the presence of Mg^{2+} at each time minus the Δ fluorescence in presence of Ca^{2+} at the corresponding time. The values were normalized to 100 μg of protein and expressed as percentage of the respective value at 0 time. The results are the average of at least three independent experiments and 7–9 animals were used for each diet group

After densitometric analysis of the scanned membranes the results were quantitatively expressed as density arbitrary units/100 μg protein (Fig. 4).

Urothelial Endocytic Vesicles Fatty Acid Composition

The changes of lipid membrane composition under the diet treatments were corroborated by the fatty acid analysis of the respective vesicles preparations and are shown in Table 1. There were no significant differences in the total amount of saturated fatty acids between the three diets studied. Nevertheless, the content of 16:0 and 24:0 were significantly different in OAV with respect to CV. These changes represented the decrease of very long chain fatty acids, VLCFAs (C20–C24), in favor of the increase of C16–C18 fatty acid chains. A similar changed pattern was observed when the unsaturated fatty acids were analyzed. Again, the decreased amount of very long chain unsaturated fatty acids (VLCPUFAs, C20–24) were concomitant with the increase of long chain fatty acids (LCFAs, C16–C18) in OAV. The degree of unsaturation was also differentially affected by the diet being the U/Sat ratio in OAV lower compared to the CV (3.1 ± 0.05 vs. 3.5 ± 0.013), respectively.

Discussion

For many years, it was believed that the subapical vesicle population of the urinary umbrella cells had the exclusive function to support the dramatic changes of the urine volume during filling and voiding cycle by means of membrane internalization/reinsertion processes [1]. However, the lysosome-degradative pathway has independently been shown by Zhang et al. [8] and Truschel et al. [9] in superficial umbrella cells and was recently strengthened with the demonstration of the acidified lumen of the endocytic vesicles [5]. Other authors have recently reported the development-related changes in the dynamics of endocytosis [7]. Using primary urothelial cultures, they showed that the membrane and fluid-phase endocytosis is dependent on the differentiation stage of the bladder

Journal : Large 12013 Dispatch : 19-2-2011 Pages : 12
Article No. : 9172 LE TYPESET
MS Code : CBBI-D-10-00069 CP DISK

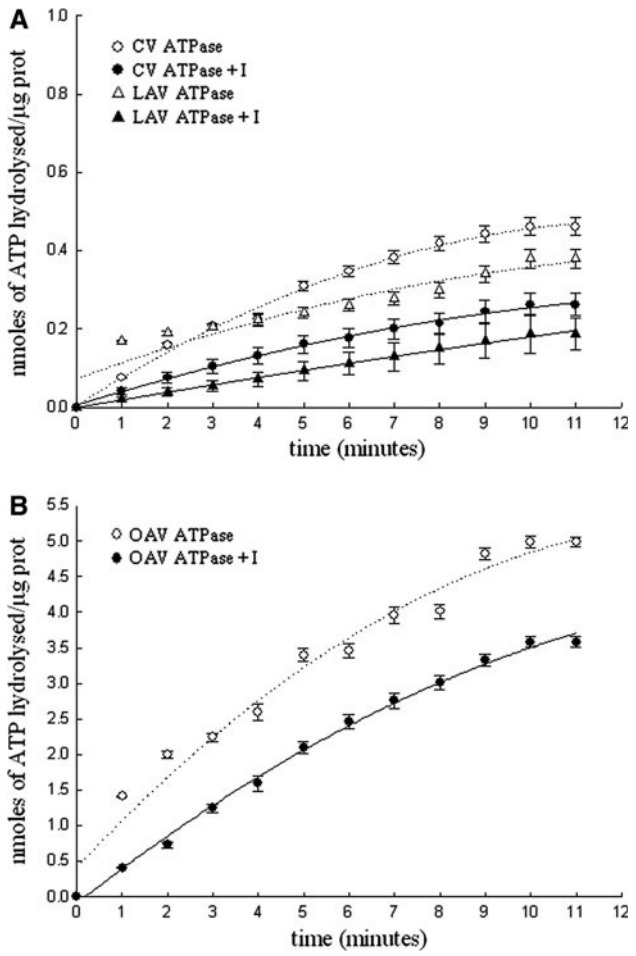

Fig. 3 V-ATPase specific activity. V-ATPase activity was measured using the linked system PK/LDH (see "Materials and Methods"). The decrease of NADH during the enzyme reaction was continuously measured in the presence and absence of P-ATPase inhibitors (I): ouabain and sodium orthovanadate by the decrease of absorbance at 340 nm. The absorbance changes (Δ Abs) of the values at 340 nm were registered at each time according to the following formula; $\Delta \text{Abs} = \text{Abs}_0 - \text{Abs}_t$; where Abs_0 corresponds to the initial absorbance and Abs_t the absorbance at the indicate times. Finally the nmoles of ATP hydrolyzed, obtained from the absorbance changes, were plotted as: nmoles of ATP hydrolyzed/µg protein as a function of the indicated times. **a** the kinetics of the ATP hydrolysis of CV and LAV (*filled symbols*) were similar with a specific activity of about 0.02 nmoles of ATP hydrolyzed/µg, protein/min. **b** the hydrolytic activity shown by OAV (*filled symbols*) was 0.3 nmoles of ATP hydrolyzed/µg, protein/min. The latter represents about 10.0 times more activity than that of CV ($P < 0.05$, ANOVA-Bonferroni test). The background activity (determined in the absence of ATP) was subtracted from all of the values shown

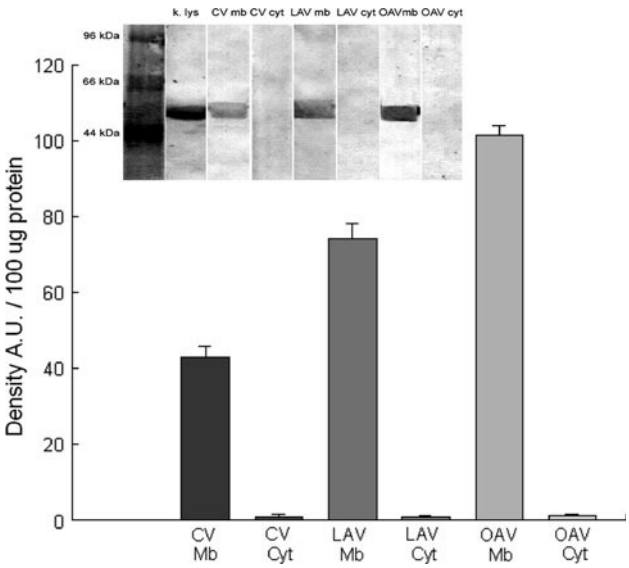

Fig. 4 Topological assembly of V-ATPase domains. **a** The assembly of the V_1 and V_0 domains was determined by monitoring the 56 kDa subunit B of V_1 domain on both, vesicles and cytosol ("soluble") fractions (see "Materials and Methods"). Western Blotting was performed with the primary antibody V-ATPase B1/2 (1:200) at 4°C) and Anti-Rabbit Ig horseradish-peroxidase conjugated (1:500) as secondary antibody. Strong positive mark was always found in the membrane fraction (*Mb*) of all three vesicles probed: CV, LAV, and OAV. Only a very light positive mark in the corresponding cytosolic (*Cyt*) fractions was observed. Kidney lysate (*k lys*) was used as a positive control. Equal amounts of protein (100 µg) were seeded in each lane. **b** Densitometric analysis: the density of the bands (analyzed by the software Sigma Scan Pro 5.0, SPSS Inc. 1987–1999) were expressed as density (arbitrary units)/100 µg protein

superficial urothelial cells. These authors reported a decrease of 43% of fluid-phase endocytosis as well as a decrease of about 85% of membrane-bound endocytosis in highly differentiated superficial urothelial cells. It is likely that the endocytic compartment studied by us is not quantitatively comparable to that of Kreft et al. [7] since a stretch-induced endocytosis was obtained in the experimental system whereas the constitutive apical endocytosis without mechanical stimuli in superficial urothelial cells was studied by Kreft et al.

This prompted to investigate the membrane permeability [10] and the ATPase-dependent acidification of the uroepithelial subapical vesicles to get insight into possible mechanisms of urinary bladder cancer development induced by urine content. We have systematically studied the structural and functional roles of lipids on the dynamic properties of the umbrella cell epithelium. The results concerning physical properties [12] as well as the structural analysis [14] of the endocytic vesicle membrane, always exhibited a dependence on the membrane lipid composition [11, 13]. More recently, we showed the leakage of the endocytosed fluid marker (HPTS) out of the endocytic vesicle lumen [10]. This process, a new alternative route of the endocytic trafficking during the bladder voiding/filling cycle, was again dependent on the membrane lipid composition. The lysosomal degradative pathway described [9] implies the presence of a proton pump V-ATPase responsible for the organelle acidification process. It was of particular interest to know whether the V-pump, through the regulation of the

Journal : Large 12013 Dispatch : 19-2-2011 Pages : 12
Article No. : 9172 LE TYPESET
MS Code : CBBI-D-10-00069 CP DISK

Table 1 Endocytic vesicles fatty acid composition

Diet	CV	LAV	OAV
Fatty acids			
Saturated			
14:0	1.52 ± 0.99	2.46 ± 0.58	1.11 ± 0.37
16:0	11.34 ± 3.79	13.06 ± 3.86	18.25 ± 2.43
18:0	15.84 ± 2.85	12.63 ± 1.66	15.70 ± 2.75
20:0	ND	0.28 ± 0.02	ND
22:0	ND	ND	0.61 ± 0.12
24:0	11.01 ± 7.42	15.47 ± 1.57	3.43 ± 0.44
Unsaturated			
14:1	2.47 ± 0.96	3.26 ± 0.31	2.36 ± 0.98
16:1	0.46 ± 0.12	1.43 ± 0.98	1.07 ± 0.04
18:1 N9	12.02 ± 3.51	10.24 ± 3.54	17.77 ± 0.45
18:2 N6	11.73 ± 1.67	9.24 ± 1.15	13.73 ± 0.18
18:3 N6	0.82 ± 0.24	4.89 ± 1.35	3.94 ± 1.22
18:3 N3	0.33 ± 0.12	0.48 ± 0.12	ND
20:1 N9	2.40 ± 1.69	3.10 ± 0.98	6.05 ± 1.04
20:2 N9	0.60 ± 0.12	5.29 ± 1.33	2.53 ± 0.82
20:3 N9	ND	6.02 ± 2.30	0.59 ± 0.01
20:4 N6	0.48 ± 0.18	10.43 ± 2.30	10.39 ± 3.27
20:3 N3	22.36 ± 6.55	0.70 ± 0.25	0.14 ± 0.06
22:1 N9	ND	0.15 ± 0.01	0.48 ± 0.02
20:5 N3	6.56 ± 2.95	0.78 ± 0.09	1.76 ± 0.50
22:6 N3	ND	ND	ND
24:1	ND	ND	ND
Sat %	39.72 ± 1.98	43.92 ± 3.39	39.13 ± 0.19
Unsat %	60.27 ± 1.34	56.07 ± 9.03	60.86 ± 0.42
DB U/Sat	3.51 ± 0.01	3.27 ± 0.49	3.18 ± 0.05
N9	30.87 ± 3.80	37.84 ± 3.03	43.15 ± 4.53
N6	13.04 ± 2.28	24.57 ± 2.82	28.07 ± 0.14
N3	29.26 ± 2.38	1.96 ± 0.39	1.90 ± 0.56
N6/N3 ratio	0.44 ± 0.01	1.47 ± 0.23	15.42 ± 4.61
VLC PUFAs	30.01 ± 2.63	23.24 ± 4.82	12.93 ± 2.45
LC–VLC MUFAs	14.42 ± 1.28	13.50 ± 4.38	24.32 ± 2.38
LCFA (C16–18)	52.56 ± 2.38	52.01 ± 4.39	70.48 ± 2.39
VLCFA (C20–24)	43.43 ± 3.68	42.26 ± 1.39	26.03 ± 4.39

Esters of fatty acids prepared from the endocytic were analyzed by gas chromatography. Values (average of three experiments) are expressed as % of total fatty acid contents ± SEM. *ND* not detected; *DB U/sat* % of each fatty acid *x* number of double bonds/% of saturated fatty acid; N9, N6, and N3 are the family derivatives, respectively. *VLC PUFAs* very long chain polyunsaturated fatty acids; *LC–VLC MUFAs* long-chain + very long chain monounsaturated fatty acids; *LC FA* long chain fatty acids, 16–18 carbons; *VLC FA* very long chain fatty acids, 20–24 carbons. Between 7–9 animals were used for each diet group

acidification process, may function as a biochemical switch controlling the "sorting" transport along the endocytosis routes cited. Thus, the aim in this study was to find some biophysico-chemical tools to modulate the V-ATPase activity "in vivo", offering the possibility for future studies of the effects of enzyme activities in the endocytic pathways. The V-ATPase, similar to other membrane proteins, can be affected by the lipid molecules that surround it; therefore, we decided to study both the catalytic and proton-translocase activities of the urothelial V-ATPase in membranes bearing different lipid compositions as a consequence of dietary treatment. First, it was confirmed that V-ATPase was present in both, plasma membrane and intracellular vesicles of the superficial umbrella cells, in all three diet-differentiated urothelia (CV, LAV, and OAV) (Fig. 1). When the proton translocation activity was studied in the presence of Mg^{2+}, the OAV could be clearly distinguished from the CV and LAV for its delayed acidification rate (Fig. 2). Several mechanisms are feasible for controlling the V-ATPase function. Among those, the more extensively studied are the reversible physical dissociation of the V_1 and V_0 domains and the changes in the functional coupling efficiency of proton transport and ATP hydrolysis [17]. Then we decided to investigate three possible causes for the differential kinetic behavior of OAV: the state of assembly/disassembly of the V_0 –V_1 complex (physical dissociation), the coupling state of the V_0 –V_1 complex, and the enzyme density in the membrane [17, 29]. The physical association between V_1 and V_0 is essential, but not sufficient, for the functional coupling of V-pump. Ca^{2+} but not Mg^{2+}, is able to induce the functional uncoupling, (with the consequent decrease of proton translocation) without the topological disassembly of the two V-ATPase domains, V_0 and V_1 [18]. Using this advantageous differential cation effect on the V-ATPase function, we also explored the coupling state of the V-ATPase domains performing the proton transport assay in the presence of Ca^{2+} as compared to Mg^{2+}. The results (Fig. 2) showed that the Mg^{2+} substitution partially inhibited proton translocation in CV and LAV thus confirming the uncoupling ability of the Ca^{2+} on the V-ATPase-complex. Nevertheless, the uncoupling effect of Ca^{2+} was not seen in OAV. Keeping in mind that the kinetics of proton translocation, as observed by the proton concentration in the lumen of the vesicle, is the result of an interplay between V-ATPase activity, proton permeability ,and probably proton countertransport, we uncoupled the V-ATPase by the addition of Ca^{2+} in an attempt to determine the level of proton translocation in the absence of the V-ATPase activity. Thus, under such condition, and assuming that the proton concentration basal level obtained is independent of the V-ATPase activity, the latter can be subtracted from the total proton concentration (in presence of Mg^{2+}) and the "true" V-ATPase proton translocation can be deduced (Fig. 2). The results shown in Fig. 2 indicate that the V-ATPase is being totally or partially uncoupled by Ca^{2+} whereas no significant fluorescence emission change was observed in the "true" V-ATPase of OAV suggesting that the native state of the

Journal : Large 12013 Dispatch : 19-2-2011 Pages : 12
Article No. : 9172 LE TYPESET
MS Code : CBBI-D-10-00069 CP DISK

V_0 –V_1 complex is at least partially uncoupled in these vesicles which is probably the cause of the deficient proton transport observed in OAV. When we studied the ATP hydrolytic activity of the vesicle suspensions, the catalytic activity in OAV was about 10 times higher than CV and LAV (Fig. 3). The lack of correlation between the increased ATPase hydrolytic activity and the reduced proton translocation was another indication of some degree of uncoupling or slippage phenomenon analogous to that observed in P-ATPase type ion pumps [30]. The Western-blotting analysis performed to further explore the disassembling of the V_0 –V_1 complex revealed that the B subunit of the V_1 domain was in a membrane-bound state in all the membranes studied and that the cytosol fraction lacks free V_1 units (Fig. 4). Together, the results argue in favor of a functionally rather than structurally uncoupled state of the V-ATPase pump in OAV which was related to the particular membrane lipid composition of these vesicles. The mechanism underlying this slippage is not clear, but changes of lipid composition could induce a conformational change in the proton channel resulting in impaired proton flow. As a compensatory mechanism, the V-ATPase pump functioning as a "pH sensor" [31] initiates the increase of ATP hydrolysis in a futile cycle. The lipid disorganizing effect on this membrane protein seems to be plausible since various ultrastructural changes that we have already reported occur in OAV compared to CV and LAV [13, 14]. We have shown that the olein-diet promoted the lowest fluoresce anisotropy of the membrane urothelium when compared with membranes derived from control or corn-oil diet indicating a decreased lipid rigidity [14]. These results correlated with changes of the structural organization observed after morphometric analysis of EM images negatively stained. They showed a statistically significant increase of the minimal hexagonally packed particles size as well as an increased interparticle spacing. Two other distances, the space between two hexagonal packed particle arrays and that between two neighboring super-arrays were also observed to be higher in the olein-diet membrane when compared with the control and corn-oil membrane [14]. It was concluded that the lipid matrix surrounding the uroplakin particles imposed by the olein diet may be "looser" than that of the control or corn-oil diet.

As an alternative explanation we consider that the membrane permeability alteration in OAV, reflected by a preferential leakage of negatively charged ions or molecules, as evidenced by the anionic HPTS fluorescent probe [10], could generate a relative deficit of positive charges on the exoplasmic side creating an electrical transmembrane potential which could finally be inhibitory for inward proton pumping activity. By contrast, in CV and LAV, no preferential leakage of the anionic HPTS was observed [10]. Thus, the protonization of HPTS may generate a proton deficiency maintaining the proton pumping of the V-ATPase. It is possible to speculate, even if we do not have experimental support as yet, an increased proton leakage throughout FFAs (free fatty acids) flip across the membrane in a protonated state as a proton back-transport. Contrary to the membrane organization observed in CV and LAV, the olive-oil-rich diet may change the membrane permeability in OAV, thus inducing a lipid dependent unfavorable membrane potential with the consequent inhibition of proton translocation while increasing the ATPase activity. Even if the insertion of higher amount of V-ATPase (Fig. 4) could be involved in the increased hydrolytic ATPase activity observed in OAV, this would not be favorable for increasing concomitantly the proton pumping activity. The absence of free V_1 domain in the cytoplasmic fraction of all three membranes studied is an evidence that the assembled/disassembled (physical association) state of urothelial V-ATPase is not affected by the lipid environment.

The polar head group and the fatty acyl chain regions can also alter the protein structural conformation and therefore its functioning [32]. The complexity of effects induced on the protein functions by the bilayer lipid composition may be varied and we have only considered those directly emerging from the results. One important property of the lipid bilayer is the thickness of the hydrophobic core since many membrane protein activities respond differently to hydrophobic mismatch; in general the highest activities are observed with a chain length of about C18, with lipids with shorter or longer chains supporting lower activities [33, 34]. The behavior of proton translocation of the urothelial membranes studied seems to follow such general profile since the lower activity observed in OAV compared with CV and LAV was concomitant with a decrease in the content of longer fatty acyl chain length (see Table 1). Nevertheless, if the protein conformational change is such that the hydrophobic thickness of the protein is greater than that of the lipid, a stretching of the lipids in the vicinity of the protein would be necessary. The particular membrane conformation adopted by lipids of OAV might thus not be optimal for a proper proton pump function. An interesting report in this regard is that of Chung [19] for the requirement of C26 acyl group for a fully functional V-ATPase that correlates with the decreased percentage of VLCFAs and the impairment of vacuolar acidification observed in the OAV membranes.

By dietary manipulation, we have developed an experimental biological–biochemical system in which a differential functional coupling of V-ATPase could be effectively established. With different methodologies, we have previously shown [10–14] that an oleic acid-rich diet induces a disorganized vesicular membrane of the urothelium which

Journal : Large 12013 Dispatch : 19-2-2011 Pages : 12
Article No. : 9172 LE TYPESET
MS Code : CBBI-D-10-00069 CP DISK

correlates with the results of this study reporting an uncoupled state of the V-ATPase in this membrane. Furthermore, the results describe for the first time that different lipid-dependent coupled/uncoupled states of the V-ATPase may be studied in the natural vesicles thus contributing to the understanding on how this enzyme may respond to different lipid environment. This experimental approach may also be applicable to study the effect of coupling-related potential factors such as those of toxic compounds, present in the urine and with possibilities to be internalized into the umbrella cells.

Acknowledgments This study was supported by grants from SECYT-UNC and CONICET, Argentina. E.J. Grasso is a doctoral fellow of CONICET, Argentina. We are grateful to Mariana Piegari and Gina Mazzudulli for their technical assistance and to Dr. Pietro Ciancaglini for the kind gift of P-ATPase inhibitors.

References

1. Hicks, M. (1975). The mammalian urinary bladder: An accommodating organ. *Biological Review, 50*, 215–246.
2. Lewis, S. A. (2000). Everything you wanted to know about the bladder epithelium but were afraid to ask. *American Journal of Physiology, 278*, F867–F874.
3. Khandelwal, P., Ruiz, W. G., & Apodaca, G. (2010). Compensatory endocytosis in bladder umbrella cells occurs through an integrin-regulated and RhoA- and dynamin-dependent pathway. *The EMBO Journal, 29*, 1961–1975.
4. Apodaca, G. (2004). The uroepithelium: Not just a passive barrier. *Traffic, 5*, 117–128.
5. Guo, X., Tu, L., Gumper, I., Plesken, H., Novak, E. K., Chintala, S., et al. (2009). Involvement of Vps33a in the fusion of uroplakin-degrading multivesicular bodies with lysosomes. *Traffic, 10*(9), 1350–1361.
6. Kreft, M. E., Jezernik, K., Kreft, M., & Romih, R. (2009). Apical plasma membrane traffic in superficial cells of bladder urothelium. *Annals of the New York Academy of Sciences, 1152*, 18–29.
7. Kreft, M. E., Romih, R., Kreft, M., & Jezernik, K. (2009). Endocytotic activity of bladder superficial urothelial cells is inversely related to their differentiation stage. *Differentiation, 77*, 48–59.
8. Zhang, S. X., & Seguchi, H. (1994). The fate of the luminal asymmetric unit membrane of the superficial cell of the rat transitional epithelium. *Histology and Histopathology, 9*, 315–323.
9. Truschel, S. T., Wang, E., Ruiz, W. G., Leung, S. M., Rojas, R., Lavelle, J., et al. (2002). Stretch-regulated exocytosis/endocytosis in bladder umbrella cells. *Molecular Biology of the Cell, 13*, 830–846.
10. Grasso, E. J., & Calderon, R. O. (2009). Urinary bladder membrane permeability differentially induced by membrane lipid composition. *Molecular and Cellular Biochemistry, 330*, 163–169.
11. Calderon, R. O., Glocker, M., & Eynard, A. R. (1998). Lipid and fatty acid composition of different fractions from rat urinary transitional epithelium. *Lipids, 33*, 1017–1022.
12. Calderon, R. O., & Eynard, A. R. (2000). Fatty acids specifically related to anisotropic properties of plasma membranes from rat urothelium. *Biochimica et Biophysica Acta, 1483*, 174–184.
13. Bongiovanni, G. A., Eynard, A. R., & Calderón, R. O. (2005). Altered lipid profile and changes in uroplakin properties of rat urothelial plasma membrane with diets of different lipid composition. *Molecular and Cellular Biochemistry, 271*(1–2), 69–75.
14. Calderon, R. O., & Grasso, E. J. (2006). Symmetric array of the urothelium surface controlled by the lipid lattice composition. *Biochemical and Biophysical Research Communications, 339*, 642–646.
15. O'Callaghan, K. M., Ayllon, V., O'Keeffe, J., Wang, Y., Cox, O. T., Loughran, G., et al. (2010). Heme-binding protein HRG-1 is induced by insulin-like growth factor I and associates with the vacuolar H+-ATPase to control endosomal pH and receptor trafficking. *The Journal of Biological Chemistry, 285*(1), 381–391.
16. Tomochika, K., Shinoda, S., Kumon, H., Mori, M., Moriyama, Y., & Futai, M. (1997). Vacuolar-type H(+)-ATPase in mouse bladder epithelium is responsible for urinary acidification. *FEBS Letters, 404*(1), 61–64.
17. Cipriano, D. J., Wang, Y., Bond, S., Hinton, A., Jefferies, K. C., Qi, J., et al. (2008). Structure and regulation of the vacuolar ATPases. *Biochimica et Biophysica Acta, 1777*, 599–604.
18. Crider, B. P., & Xie, X. S. (2003). Characterization of the functional coupling of bovine brain Vacuolar-type H^+-translocating ATPase. *The Journal of Biological Chemistry, 278*(45), 44281–44288.
19. Chung, J. H., Lester, R. L., & Dickson, R. C. (2003). Sphingolipid requirement for generation of a functional V_1 component of the vacuolar ATPase. *The Journal of Biological Chemistry, 278*(31), 28872–28881.
20. Straubinger, R. M., Papahadjopoulos, D., & Hong, K. (1990). Endocytosis and Intracellular fate of liposomes using pyranine as a probe. *Biochemistry, 29*, 4929–4939.
21. Chang, A., Hammond, T. G., Sun, S. T., & Zeidel, M. L. (1994). Permeability properties of the mammalian bladder apical membrane. *American Journal of Physiology, 267*, 1483–1492.
22. Lewis, S., & de Moura, J. (1982). Incorporation of cytoplasmic vesicles into apical membrane of mammalian urinary bladder epithelium. *Nature, 297*, 685–688.
23. de Lima Santos, H., Lopes, M. L., Maggio, B., & Ciancaglini, P. (2005). Na, K-ATPase reconstituted in liposomes: Effects of lipid composition on hydrolytic activity and enzyme orientation. *Colloids and Surfaces B: Biointerfaces, 41*, 239–248.
24. Kane, P. M., Kuehn, M. C., Howald-Stevenson, I., & Stevens, T. H. (1992). Assembly and targeting of peripheral and integral membrane subunits of the yeast vacuolar H^+-ATPase. *The Journal of Biological Chemistry, 267*(1), 447–454.
25. Folch, J., Lees, M., & Stanley, G. H. (1957). A simple method for the isolation and purification of total lipids from animal tissues. *The Journal of Biological Chemistry, 226*, 497–508.
26. Cantellops, D., Reid, A. P., Eitenmiller, R. R., & Long, A. R. (1999). Determination of lipids in infant formula powder by direct extraction methylation of lipids and fatty acid methyl esters (FAME) analysis by gas chromatography. *Journal of AOAC International, 82*, 1128–1139.
27. Lowry, R. O. H., Rosebrough, N. J., Farr, A. L., & Randall, R. J. (1951). Protein measurement with the Folin phenol reagent. *The Journal of Biological Chemistry, 193*, 265–275.
28. Overly, C. C., Lee, K. D., Berthiaume, E., & Hollenbeck, P. J. (1995). Quantitative measurement of intraorganelle pH in the endosomal-lysosomal pathway in neurons by using ratiometric imaging with pyranine. *Proceedings of the National Academy of Sciences of the United States of America, 92*(8), 3156–3160.
29. Lafourcade, C., Sobo, K., Kieffer-Jaquinod, S., Garin, J., & van der Goot, F. G. (2008). Regulation of the V-ATPasa along the endocytic pathway occurs through reversible subunit association and membrane localization. *Plos One, 3*(7), e2758.
30. Sumbilla, C., Lewis, D., Hammerschmidt, T., & Inesi, G. (2002). The slippage of the Ca^{2+} pump and its control by anions and

Journal : Large 12013 | Dispatch : 19-2-2011 | Pages : 12
Article No. : 9172 | LE | TYPESET
MS Code : CBBI-D-10-00069 | CP | DISK

curcumin in skeletal and cardiac sarcoplasmic reticulum. *The Journal of Biological Chemistry, 277*(16), 13900–13906.
31. Shao, E., & Forgac, M. (2004). Involvement of the nonhomologous region of subunit A of the yeast V-ATPase in coupling and in vivo dissociation. *The Journal of Biological Chemistry, 279*, 48663–48670.
32. Lee, A. G. (2004). How lipids affect the activities of integral membrane proteins. *Biochimica et Biophysica Acta, 1666*, 62–87.
33. Caffrey, M., & Feigenson, G. W. (1981). Fluorescence quenching in model membranes: 3 Relationship between calcium adenosinetriphosphatase enzyme activity and the affinity of the protein for phosphatidylcholine with different acyl chain characteristics. *Biochemistry, 20*, 1949–1961.
34. Lee, A. G. (2003). Lipid-protein interactions in biological membranes: A structural perspective. *Biochimica et Biophysica Acta, 1612*, 1–40.

Journal : **Large 12013** Dispatch : **19-2-2011** Pages : **12**
Article No. : **9172** ☐ LE ☐ TYPESET
MS Code : **CBBI-D-10-00069** ☑ CP ☑ DISK